



This discussion paper is/has been under review for the journal Geoscientific Model Development (GMD). Please refer to the corresponding final paper in GMD if available.

# A dynamic probability density function treatment of cloud mass and number concentrations for low level clouds in GFDL SCM/GCM

H. Guo<sup>1</sup>, J.-C. Golaz<sup>2</sup>, L. J. Donner<sup>2</sup>, V. E. Larson<sup>3</sup>, D. P. Schanen<sup>3</sup>, and B. M. Griffin<sup>3</sup>

<sup>1</sup>UCAR Visiting Scientist Programs, NOAA/Geophysical Fluid Dynamics Laboratory, Princeton, New Jersey, USA

<sup>2</sup>NOAA/Geophysical Fluid Dynamics Laboratory, Princeton, New Jersey, USA

<sup>3</sup>Atmospheric Science Group, Department of Mathematical Sciences, University of Wisconsin-Milwaukee, Milwaukee, Wisconsin, USA

Received: 27 April 2010 – Accepted: 28 April 2010 – Published: 11 May 2010

Correspondence to: H. Guo (huan.guo@noaa.gov)

Published by Copernicus Publications on behalf of the European Geosciences Union.

**GMDD**

3, 541–568, 2010

**Dynamics-PDF in  
GFDL SCM-CLUBB**

H. Guo et al.

Title Page

Abstract

Introduction

Conclusions

References

Tables

Figures

⏪

⏩

◀

▶

Back

Close

Full Screen / Esc

Printer-friendly Version

Interactive Discussion



## Abstract

Successful simulation of cloud-aerosol interactions (indirect aerosol effects) in climate models requires relating grid-scale aerosol, dynamic, and thermodynamic fields to small-scale processes like aerosol activation. A turbulence and cloud parameterization, based on multivariate probability density functions (PDFs) of sub-grid vertical velocity, temperature, and moisture, has been extended to treat aerosol activation. This dynamics-PDF approach offers a solution to the problem of the scale gap between the resolution of climate models and the scales relevant for aerosol activation and a means to overcome the limitations of diagnostic estimates of cloud droplet number concentration based only on aerosol concentration.

Incorporated into a single-column model for GFDL AM3, the dynamics-PDF parameterization successfully simulates cloud fraction and water content for shallow cumulus, stratocumulus, and cumulus-under-stratocumulus regimes. The extension to treat aerosol activation predicts droplet number concentrations in good agreement with large eddy simulation (LES). The dynamics-PDF droplet number concentrations match LES results more closely than state-of-the-science diagnostic relationships between aerosol concentration and droplet number concentration.

## 1 Introduction

Low-level clouds have been identified as one of largest uncertainties in estimating climate sensitivity (Webb et al., 2006; Forster et al., 2007). The motions driving microphysics in boundary layer clouds are mostly sub-grid scale in climate and numerical weather prediction (NWP) models (Stull, 1988). Boundary layer clouds are diverse, comprising cumulus, stratocumulus, cumulus-under-stratocumulus, and others. As a result, boundary layer representations have been challenging and formidable problems for decades (Randall et al., 2000). Moreover, the global coverage and large grid spacing of general circulation models (GCMs) introduce additional difficulties to represent boundary layer processes in a *unified* parameterization package.

**GMDD**

3, 541–568, 2010

## Dynamics-PDF in GFDL SCM-CLUBB

H. Guo et al.

Title Page

Abstract

Introduction

Conclusions

References

Tables

Figures

⏪

⏩

◀

▶

Back

Close

Full Screen / Esc

Printer-friendly Version

Interactive Discussion



**Dynamics-PDF in  
GFDL SCM-CLUBB**

H. Guo et al.

[Title Page](#)[Abstract](#)[Introduction](#)[Conclusions](#)[References](#)[Tables](#)[Figures](#)[I◀](#)[▶I](#)[◀](#)[▶](#)[Back](#)[Close](#)[Full Screen / Esc](#)[Printer-friendly Version](#)[Interactive Discussion](#)

Cloud-aerosol interactions are an especially important aspect of the role of low clouds in climate and climate sensitivity (Heintzenberg and Charlson, 2009). Aerosol activation depends on local super-saturation (and, subsequently, vertical velocity) at scales far below those resolved in climate and NWP models. Application of robust, physically based activation theory using dynamic and thermodynamic fields at the coarse resolution of these models is highly problematic due to the nonlinear dependence of activation on vertical velocity. Vertical velocity typically exhibits large sub-grid variability, evident in observations and process models for both convective and stratiform clouds (Leary and Houze, 1980; Donner et al., 1999; Stevens et al., 2005). In face of these conceptual difficulties, aerosol activation in climate models is often parameterized using diagnostic relationships between aerosol concentration and droplet number concentration (Boucher and Lohmann, 1995). These diagnostic approaches have merits in the absence of a satisfactory solution to the problem of the scale gap between the resolution of climate and NWP models and the scales relevant for aerosol activation. However, these approaches are limited in that they fail to account for controls on activation that are well-established in theory, especially variations in super-saturation related to vertical velocity. Considerable scatter characterizes the relationships between aerosol concentration and droplet number concentration (e.g., Ramanathan et al., 2001, Fig. 5), inevitably, given important controls beyond aerosol concentration on droplet number concentration.

We have incorporated a higher-order turbulence closure parameterization scheme into the single column version of the next generation of the GFDL Atmospheric GCM (AM3) (Donner et al., 2010). This boundary layer scheme is a partial third-order turbulence closure scheme. It uses a dynamic multi-variate probability density function (dynamics-PDF) to represent the sub-grid variability in vertical velocity, liquid water potential temperature, and total water content in a model grid box (Golaz, 2001; Golaz et al., 2002a, b, 2007; Larson et al., 2002; Larson and Golaz, 2005). Although PDFs representing sub-grid variations in moisture and/or temperature have been employed in the past for the parameterization of fractional cloudiness (Mellor, 1977),

parameterizations that include joint variations in vertical velocity are rare (Lappen and Randall, 2001). The inclusion of the vertical velocity offers the advantage of tying thermodynamics and dynamics together; and in so doing, a consistent framework can be created for representing clouds and their associated boundary layer turbulent transport and/or mixing.

Because this dynamics-PDF parameterization treats temperature, moisture, and vertical velocity consistently, it also offers the possibility of treating aerosol activation process more realistically. The vertical velocity is important for aerosol activation through super-saturation. As noted above, the dynamics-PDF approach is a potential solution to the problem of the scale gap between the resolution of GCMs and the scales relevant for aerosol activation. One purpose of this paper is to describe additions to the dynamics-PDF parameterization to enable it to parameterize cloud droplet number, a capability it does not currently have. In addition to using the PDF of vertical velocity directly for aerosol activation, we further incorporated the turbulent transport of cloud droplet number concentration ( $N_d$ ) in the dynamics-PDF scheme.  $N_d$  is predicted via a budget equation (Ghan et al., 1997; Lohmann et al., 1999; Ming et al., 2007; Morrison and Gettelman, 2008). This budget equation includes the turbulent and large-scale transport of  $N_d$ , source terms such as aerosol activation (Ming et al., 2006), and sink terms such as evaporation (Ovtchinnikov and Ghan, 2005).

This paper evaluates the performance of the dynamics-PDF scheme within the framework of the GFDL single column model (SCM), because the SCM configuration is an efficient framework for implementing and performing the initial evaluations of new physical packages without the complexity of a full GCM. Since we mainly investigate boundary layer clouds in this study, we apply the dynamics-PDF scheme in the lowest 4 km of the atmosphere. The source code of the dynamics-PDF scheme is originally based on a single column model: cloud layers unified by binormals (CLUBB) (<http://clubb.larson-group.com>). We interfaced the GFDL SCM to CLUBB, and hereafter refer to it as GFDL SCM-CLUBB. Our main goals are twofold: 1) to improve the boundary layer representations in the GFDL SCM by incorporating the CLUBB-based

**Dynamics-PDF in  
GFDL SCM-CLUBB**

H. Guo et al.

Title Page

Abstract

Introduction

Conclusions

References

Tables

Figures



Back

Close

Full Screen / Esc

Printer-friendly Version

Interactive Discussion



dynamics-PDF parameterization, and 2) to extend the dynamics-PDF scheme to include aerosol activation. The latter is a novel application of the dynamics-PDF scheme, whose success is critical for its use in parameterizing aerosol-cloud interactions in GCMs. Caveats should be noted here. This is a first step attempting to explore aerosol effects in the GFDL SCM-CLUBB. The aerosol effects on cloud microphysical and radiative properties, and dynamics have not been interactively coupled in this study, yet.

The paper is organized as follows: Sect. 2 describes modifications made to the dynamics-PDF parameterization to incorporate the prognostic treatment of cloud droplet number concentration. Section 3 shows simulations of three representative cloud regimes (i.e., cumulus, stratocumulus, and cumulus-under-stratocumulus clouds), and evaluates them against large eddy simulations (LES) and available observations. Section 4 provides conclusions and describes future work.

## 2 Prognostic equation for droplet number concentration

A mechanistic activation parameterization, based on Köhler theory, requires vertical velocity. The need to parameterize sub-grid variation of vertical velocity is especially evident, when the grid mean vertical velocity is negative or zero, but both small-scale upward and downward motions are present. For example, stratocumulus regimes occur in environments with large-scale subsidence. Sub-grid scale updrafts become critical for the existence of these prevailing stratocumulus clouds. The dynamics-PDF parameterization directly provides the vertical velocity PDF that is required to drive aerosol activation. Furthermore, the prediction of the sub-grid variation of vertical velocity is consistently combined with the predictions of temperature and moisture (Larson and Golaz, 2005).

The GFDL AM3 has incorporated a mechanistic aerosol activation scheme developed by Ming et al. (2006). The aerosol activation scheme provides an initial cloud droplet number concentration. Cloud droplets are also subjected to turbulent

---

### Dynamics-PDF in GFDL SCM-CLUBB

H. Guo et al.

---

Title Page

Abstract

Introduction

Conclusions

References

Tables

Figures



Back

Close

Full Screen / Esc

Printer-friendly Version

Interactive Discussion



transport and/or mixing, evaporation, collision and/or coalescence, and other physical processes. To explore the effects of aerosols on low-level clouds, we have also incorporated the treatment of turbulent transport and/or mixing of the cloud droplet number concentration in the dynamics-PDF scheme. The prognostic equation for the droplet number concentration is as follows:

$$\frac{\partial \overline{N_d}}{\partial t} = -\overline{w} \frac{\partial \overline{N_d}}{\partial z} - \frac{\partial}{\partial z} \overline{w'N'_d} + S - A - C - E \quad (1)$$

where  $\overline{N_d}$  is the layer-averaged droplet number concentration,  $\overline{w} \frac{\partial \overline{N_d}}{\partial z}$  is the large-scale transport of cloud droplets and  $\overline{w}$  is an imposed large-scale vertical velocity,  $\frac{\partial}{\partial z} \overline{w'N'_d}$  is the turbulent transport of cloud droplets,  $S$  denotes a droplet source term due to aerosol activation, and  $A$ ,  $C$ , and  $E$  denote droplet sink terms due to autoconversion, collection by rain drops, and evaporation, respectively.

The turbulent transport of droplets concentration ( $\frac{\partial}{\partial z} \overline{w'N'_d}$ ) is approximated by diffusing downgradient in-cloud droplet number concentration ( $\overline{N_d^c}$ ) weighted by the cloud fraction as follows:

$$\begin{aligned} -\frac{\partial}{\partial z} \overline{w'N'_d} &= -\frac{\partial}{\partial z} \left( CF \overline{w'^c N_d'^c} \right) \\ &= \frac{\partial}{\partial z} \left( CF \cdot D \frac{\partial}{\partial z} \overline{N_d^c} \right) \end{aligned}$$

where  $\overline{(\ )}$  denotes an average over cloudy region,  $(\ )^c$  denotes the in-cloud perturbation from the in-cloud average,  $CF$  denotes the cloud fraction, and  $D$  denotes eddy diffusivity.

Title Page

Abstract

Introduction

Conclusions

References

Tables

Figures

◀

▶

◀

▶

Back

Close

Full Screen / Esc

Printer-friendly Version

Interactive Discussion



If we substitute  $\overline{N_d^c} = \overline{N_d}/CF$ , then

$$-\frac{\partial \overline{w'N_d'}}{\partial z} = \frac{\partial}{\partial z} \left[ D \cdot \left( \frac{\partial \overline{N_d}}{\partial z} - \frac{\overline{N_d}}{CF} \frac{\partial CF}{\partial z} \right) \right]$$

$$= \frac{\partial}{\partial z} \left( D \frac{\partial \overline{N_d}}{\partial z} \right) - \frac{\partial}{\partial z} \left( D \frac{\overline{N_d}}{CF} \frac{\partial CF}{\partial z} \right)$$

5 The first term represents the diffusion of the layer-averaged droplet number concentration,  $\overline{N_d}$ . The second term is a correction term that accounts for the change of CF with height. The discretization form is as follows:

$$-\left( \frac{\partial \overline{w'N_d'}}{\partial z} \right)^k = \frac{1}{z^{k+\frac{1}{2}} - z^{k-\frac{1}{2}}} \left[ D^{k+\frac{1}{2}} \frac{\overline{N_d}^{k+1} - \overline{N_d}^k}{z^{k+1} - z^k} - D^{k-\frac{1}{2}} \frac{\overline{N_d}^k - \overline{N_d}^{k-1}}{z^k - z^{k-1}} \right]$$

$$- \frac{D^{k+\frac{1}{2}}}{(z^{k+\frac{1}{2}} - z^{k-\frac{1}{2}})} \frac{\overline{N_d}^{k+1}}{\max(CF^{k+1}, CF_{\min})} \frac{CF^{k+1} - CF^k}{z^{k+1} - z^k} H(CF^{k+1} - CF^k)$$

$$- \frac{D^{k-\frac{1}{2}}}{(z^{k+\frac{1}{2}} - z^{k-\frac{1}{2}})} \frac{\overline{N_d}^{k-1}}{\max(CF^{k-1}, CF_{\min})} \frac{CF^{k-1} - CF^k}{z^k - z^{k-1}} H(CF^{k-1} - CF^k)$$

10 where  $k$  denotes the layer index, and  $H(\cdot)$  is a Heaviside step function. The Heaviside step function is introduced because the droplets transported into the clear fraction of the model grid box are assumed to be completely evaporated (Ovtchinnikov and Ghan, 2005). In order to avoid a potential division by zero, we place a lower threshold on CF ( $CF_{\min}$ ) in the denominator. As long as CF is smaller than  $CF_{\min}$ ,  $\overline{N_d}$  is set to be 0.

Title Page

Abstract

Introduction

Conclusions

References

Tables

Figures

◀

▶

◀

▶

Back

Close

Full Screen / Esc

Printer-friendly Version

Interactive Discussion



A droplet source term due to aerosol activation,  $S$ , is expressed as the difference between number concentration of droplets that can be activated and pre-existing droplet number concentration (Stevens et al., 1996; Ghan et al., 1997; Lohmann et al., 1999), that is,

$$S = \max(\overline{N_{\text{act}}} - \overline{N_{\text{d}}}, 0) / \Delta t \quad (2)$$

where  $\Delta t$  is the host SCM time step, and  $\overline{N_{\text{act}}}$  is the layer-averaged droplet number concentration due to the activation process. When new clouds form, activation occurs in updrafts. For pre-existing clouds, new droplets form if the number of activated droplets,  $\overline{N_{\text{act}}}$ , exceeds the existing droplets  $\overline{N_{\text{d}}}$ . Existing droplets completely evaporate only when the cloud dissipates (Ghan et al., 1997).

Since the activation process occurs only within saturated updrafts, and since the saturation (i.e., cloudiness) can be diagnosed based on the probability density function (PDF) of liquid potential temperature ( $\theta_l$ ) and total water content ( $q_t$ ) for clouds, we integrate over the joint PDF from the dynamics-PDF scheme to calculate  $\overline{N_{\text{act}}}$ . That is,  $\overline{N_{\text{act}}}$  is a weighted integral,

$$\overline{N_{\text{act}}} = \text{CF} \cdot \frac{\int_w \int_{\theta_l} \int_{q_t} N_{\text{act}}(w) \text{PDF}(w > 0, \text{CF}(\theta_l, q_t) > 0) dw d\theta_l dq_t}{\int_w \int_{\theta_l} \int_{q_t} \text{PDF}(w > 0, \text{CF}(\theta_l, q_t) > 0) dw d\theta_l dq_t} \quad (3)$$

The numerical integration of Eq. (3) is performed using a 64-point Gauss-Hermite quadrature for each of the Gaussian in the underlying joint-PDF.

Cloud droplet sinks due to autoconversion ( $A$ ) and collection ( $C$ ) are assumed to be linearly proportional to warm cloud mass sinks due to the corresponding processes. Note that autoconversion and collection processes are disabled in this study of non-precipitating clouds. Evaporation,  $E$ , is assumed to be linearly proportional to

Title Page

Abstract

Introduction

Conclusions

References

Tables

Figures

⏪

⏩

◀

▶

Back

Close

Full Screen / Esc

Printer-friendly Version

Interactive Discussion



the changes in cloud fraction (CF) due to the large-scale evaporation as follows:

$$E = -\min\left(\frac{\overline{N_d}}{CF} \frac{\Delta CF}{\Delta t}, 0\right). \quad (4)$$

Large-scale evaporation is consistent with the assumption that cloud droplets evaporate when the cloud dissipates.

### 3 Simulation results

To a great extent, boundary layer moist convection can be divided into three main regimes: a deep planetary boundary layer with a small cloud fraction capped by a weak inversion, a shallow planetary boundary layer with a high cloud fraction capped by a strong inversion, and an intermediate one (Stevens et al., 2001). Here we show simulation results of three cases corresponding to these representative regimes, which have been studied by the Global Energy and Water Exchange Cloud System Study (GCSS) Boundary Layer Cloud Working Group (BLCWG). These cases are also well-established benchmark cases to evaluate cloud models and boundary layer parameterizations (Stevens et al., 2001, 2005; Siebesma et al., 2003; Zhu et al., 2005). However, these cases are idealized: precipitation and shortwave radiation are neglected, and longwave radiation is highly simplified. One would argue that these idealized cases would limit the exploration of indirect aerosol effects. These cases are justified not by their idealization, but rather because they are attractive first steps in better estimating droplet number concentration in order to explore aerosol indirect effects, and evaluating the thermodynamic fields (e.g., cloud fraction and water content) consistently with the dynamic fields (e.g., vertical velocity and implicitly droplet number concentration).

These three representative cases are: 1) a trade-wind cumulus case during the Barbados Oceanographic and Meteorological Experiment (BOMEX) (Siebesma et al., 2003); 2) a non-drizzling marine stratocumulus case during the First Research Flight (RF01) of the second Dynamics and Chemistry of Marine Stratocumulus Field Study

Title Page

Abstract

Introduction

Conclusions

References

Tables

Figures

◀

▶

◀

▶

Back

Close

Full Screen / Esc

Printer-friendly Version

Interactive Discussion



---

**Dynamics-PDF in  
GFDL SCM-CLUBB**


---

H. Guo et al.

---

[Title Page](#)
[Abstract](#)
[Introduction](#)
[Conclusions](#)
[References](#)
[Tables](#)
[Figures](#)
[◀](#)
[▶](#)
[◀](#)
[▶](#)
[Back](#)
[Close](#)
[Full Screen / Esc](#)
[Printer-friendly Version](#)
[Interactive Discussion](#)


(DYCOMS-II) (Stevens et al., 2005); and 3) a cumulus-under-stratocumulus case during the Atlantic Trade Wind Experiment (ATEX) (Stevens et al., 2001). The first case is a typical trade wind cumulus cloud with a low cloud fraction of about 5%, hereafter referred to as BOMEX. It was capped by a weak inversion of potential temperature and moisture (i.e., specific humidity) inversion strengths of  $0.007 \text{ K m}^{-1}$  and  $-0.008 \text{ g kg}^{-1} \text{ m}^{-1}$ , respectively. The second case is a nocturnal stratocumulus cloud with nearly a solid deck, hereafter referred to as RF01. RF01 was characterized by a strong inversion at cloud top. The inversion strengths of potential temperature and moisture were  $17 \text{ K m}^{-1}$  and  $-12 \text{ g kg}^{-1} \text{ m}^{-1}$ , respectively. This remarkably strong inversion requires substantially refined vertical resolution to resolve sharp gradients near cloud top. Cloud-top mixing should have led to the dissipation of the stratocumulus clouds, according to the cloud-top entrainment instability criterion (Randall, 1980). However, the observed stratocumulus clouds were stable and even slightly thickened. This makes RF01 an interesting, albeit challenging, stratiform case. BOMEX and RF01 represent two contrasting regimes and are at opposite ends of the boundary-layer moist convection spectrum. The third case is a trade-wind cumulus cloud under a relatively strong inversion, hereafter referred to as ATEX. ATEX is an intermediate case where the trade-wind cumulus cloud rises under a broken stratocumulus cloud. The cloud fraction in the cumulus layer is less than 10%, and the cloud fraction of the overlying stratocumulus layer is about 50%.

For the case configurations, we follow specifications for large eddy simulation (LES) comparison studies organized by the BLCWG (Stevens et al., 2001, 2005; Siebesma et al., 2003). Our SCM simulations are subjected to the same initial conditions and large-scale forcings as the LES. This allows for a careful evaluation of SCM simulations against the LES. Because the LES can explicitly resolve most energy-carrying eddies, they are often used as benchmark simulations. In this study, we use COAMPS<sup>1</sup> LES results as benchmark (Golaz et al., 2005). The COAMPS LES model has been modified to include an anelastic pressure solver and to add cloud droplet number concentration

<sup>1</sup>COAMPS is a registered trademark of the Naval Research Laboratory.

as a prognostic variable with the aerosol activation scheme developed by Ming et al. (2006). The entire simulation periods for BOMEX, RF01, and ATEX are 6 h, 4 h, and 8 h, respectively. To exclude the unwanted spinup behavior, we focus on simulation results over the last hour, after the simulations have reached quasi-steady states.

### 3.1 Cloud fraction and cloud water content

In Fig. 1, we compare cloud fraction (CF) and cloud water content ( $q_c$ ) from the GFDL SCM-CLUBB simulations, from COAMPS LES, and from the LES comparison ensemble and observations (if available). For the SCM-CLUBB simulations, we conducted low and high vertical resolution runs, denoted as dynamics-PDF (low-res) and dynamics-PDF (high-res), respectively. Appendix A describes the vertical grids for the host SCM and for the dynamics-PDF scheme. In the dynamics-PDF (low-res), the SCM uses low vertical resolution while the dynamics-PDF scheme uses high resolution, and they communicate via linear interpolation. In the dynamics-PDF (high-res), both the SCM and the dynamics-PDF scheme use the same high vertical resolution in the lowest 4 km (Fig. A1). The cloud fraction and  $q_c$  profiles compare favorably with those from COAMPS LES (Fig. 1), and are generally well within the LES ensemble ranges based on the LES comparison studies (Stevens et al., 2001, 2005; Siebesma et al., 2003).

In the cumulus case of BOMEX, both the dynamics-PDF (low-res) and the dynamics-PDF (high-res) simulations successfully reproduce the trade-wind cumulus cloud with a small cloud fraction and little layer-averaged cloud water content ( $q_c$ ) (Fig. 1a and b). During the last couple of hours, the simulated cloud fraction and layer-averaged  $q_c$  are in quasi-steady state. The simulated cloud fraction remains less than 6%, and the layer-averaged  $q_c$  is smaller than  $0.01 \text{ g kg}^{-1}$ .

In the stratocumulus case of RF01, the SCM-CLUBB simulations maintain a shallow but solid cloud deck (Fig. 1d).  $q_c$  increases linearly with height above the cloud base and reaches its maximum near the cloud top, similar to what was observed (Zhu et al., 2005). The simulated  $q_c$  is slightly under-estimated as compared to the COAMPS LES results, but in good agreement with the observations (Fig. 1e). Since the  $q_c$  profile is

Title Page

Abstract

Introduction

Conclusions

References

Tables

Figures

◀

▶

◀

▶

Back

Close

Full Screen / Esc

Printer-friendly Version

Interactive Discussion



sensitive to small changes in temperature and moisture caused by turbulent transport, the good agreement of  $q_c$  between the SCM-CLUBB simulations and observations implies that the dynamics-PDF scheme can properly capture the turbulent transport of temperature and moisture within the stratocumulus-topped boundary layer.

In the cumulus-under-stratocumulus case of ATEX (Stevens et al., 2001), a cumulus layer is present from 600 m to 1100 m. The cumulus cloud fraction peaks at 6% near cloud base and slightly decreases through the lower half of the cloud layer. The cloud fraction then increases to about 40% at the cloud top near the inversion (Fig. 1g). The reason is partly because the boundary layer is not dry enough to evaporate the detrained cumulus clouds, and also because the relatively strong trade inversion caps convective elements and suppresses entrainment drying. As a result, a stratocumulus layer is formed and caps the cumulus layer (Fig. 1g). The cloud fraction near the cloud top exhibits a large spread in the LES ensemble, as does the layer-averaged  $q_c$  (Fig. 1 (g) and (h)). This large spread is partially attributed to a positive feedback between the radiative cooling and the cloud moisture (Stevens et al., 2001).

For these three cases representing very different boundary layer cloud regimes, the simulations of cloud properties are generally in good agreement with the benchmark COAMPS LES, LES ensemble, and available observations. In the next section, we will apply the sub-grid variations in vertical velocity to an aerosol activation parameterization. Correlating cloud droplet number concentration ( $N_d$ ) with aerosols is necessary to study indirect aerosol effects.

### 3.2 Droplet number concentration

Figure 2 exhibits the profiles of  $N_d$  from the SCM-CLUBB simulations and from the COAMPS LES. In these simulations, the sulfate aerosol mass concentration ( $m_a$ ) is specified to be constant with height in the boundary layer. We present results with  $m_a = 1.0 \mu\text{g m}^{-3}$  and  $5.0 \mu\text{g m}^{-3}$ . The in-cloud  $N_d$  is more or less constant with height, which conforms to previous studies and observations. Consequently, the profiles of the layer-averaged  $N_d$  are similar to those of the cloud fraction (Figs. 1 and 2). As expected,

## Dynamics-PDF in GFDL SCM-CLUBB

H. Guo et al.

Title Page

Abstract

Introduction

Conclusions

References

Tables

Figures

◀

▶

◀

▶

Back

Close

Full Screen / Esc

Printer-friendly Version

Interactive Discussion



$N_d$  is higher with a higher  $m_a$  (Fig. 2). As the aerosol concentration  $m_a$  increases by a factor of 5,  $N_d$  increases by a factor of  $\sim 2$  (Table 1), indicating the greater competition for water between aerosols with a higher  $m_a$ .

$N_d$  from the SCM-CLUBB simulations agree reasonably well with those from COAMPS LES in all three cases of BOMEX, RF01, and ATEX. At a first glance, the difference between the SCM-CLUBB simulations and the COAMPS LES becomes larger at higher  $m_a$ . Although the absolute difference increases (proportionally) at higher  $m_a$ , the relative difference remains similar. The agreement for the in-cloud  $N_d$  is generally better than that for the layer-averaged  $N_d$ . The layer-averaged  $N_d$  from the SCM-CLUBB simulations is slightly under-estimated. This under-estimation tends to be alleviated in higher vertical resolution simulations (Fig. 2).

Sub-grid variability of vertical velocity is critical in these cases. Ignoring sub-grid variability would lead to negligibly small  $N_d$ , because the mean vertical velocity is negative for marine stratocumulus clouds in subtropical regions. This negligibly small  $N_d$  would obviously be unrealistic for global simulations of these prevailing stratocumulus. In addition, we calculate  $N_d$  using alternate methods that have been adopted in GCMs. One of these methods retains a mechanistic approach to aerosol activation but employs a simpler approach to generate the PDF of vertical velocity. The other uses a diagnostic relationship between aerosol concentration and  $N_d$ .

In the first alternate method, the PDF of sub-grid vertical velocity is given by a single Gaussian distribution, whose width ( $\sigma_w$ ) is diagnosed either from turbulence kinetic energy (Lohmann et al., 1999) or from vertical eddy diffusivity (Morrison and Gettelman, 2008). A lower bound ( $\sigma_{\min}$ ) is imposed on  $\sigma_w$  and often dominates  $\sigma_w$  (Golaz et al., 2010). For simplicity, we set  $\sigma_w$  to be  $\sigma_{\min}$ , and set  $\sigma_{\min}$  to be  $0.7 \text{ m s}^{-1}$  or  $2.0 \text{ m s}^{-1}$  in our sensitivity tests, and hereafter refer to this alternate as fixed  $\sigma_w$ . The second alternate method is to use an empirical relationship between the droplet number concentration and the sulfate mass concentration following Boucher and Lohmann (1995), hereafter referred to as B-L.

**Dynamics-PDF in  
GFDL SCM-CLUBB**

H. Guo et al.

Title Page

Abstract

Introduction

Conclusions

References

Tables

Figures

◀

▶

◀

▶

Back

Close

Full Screen / Esc

Printer-friendly Version

Interactive Discussion



Dynamics-PDF in  
GFDL SCM-CLUBB

H. Guo et al.

Title Page

Abstract

Introduction

Conclusions

References

Tables

Figures

◀

▶

◀

▶

Back

Close

Full Screen / Esc

Printer-friendly Version

Interactive Discussion



The vertical profiles of the in-cloud droplet number concentration averaged over the last hour for BOMEX, RF01, and ATEX are presented in Fig. 3. The in-cloud  $N_d$  are almost constant with height in the sensitivity tests of fixed  $\sigma_w$  and B-L, regardless of cumulus, stratocumulus, or cumulus-under-stratocumulus. As compared to the COAMPS LES results, the sensitivity tests of fixed  $\sigma_w$  with  $\sigma_w=0.7\text{ m s}^{-1}$  underestimate  $N_d$ . This underestimation can be alleviated by increasing  $\sigma_w$ . When  $\sigma_w$  is increased to  $2.0\text{ m s}^{-1}$ ,  $N_d$  is in good agreement with the LES results (Fig. 3 and Table 1). However, such a large  $\sigma_w$  is physically unrealistic, and the PDF of  $w$  deviates significantly from that in the LES (Fig. 4). Such a large  $\sigma_w$  is also significantly greater than what are commonly used in GCMs (Ghan et al., 1997; Donner et al., 2009; Golaz et al., 2010). Hereafter, we mainly discuss the results using  $\sigma_w=0.7\text{ m s}^{-1}$ . The tests of B-L overestimate  $N_d$  for three cases and for sulfate aerosol concentrations of  $1.0\text{ }\mu\text{g m}^{-3}$  and  $5.0\text{ }\mu\text{g m}^{-3}$ . This overestimation is consistent with other model studies (Ghan et al., 1997). Since there are no tunable parameters in the empirical relationship by Boucher and Lohmann (1995), it is hard to adjust  $N_d$  in order to match the LES results.

The relative differences of the time and space averaged  $N_d$  between the tests of fixed  $\sigma_w$  ( $\sigma_w=0.7\text{ m s}^{-1}$ ) and the COAMPS LES are about  $-30\%$ . The relative difference between the tests of B-L and the COAMPS LES can reach  $+127\%$ . The relative differences are generally smaller using the dynamics-PDF scheme than either using fixed  $\sigma_w$  ( $\sigma_w=0.7\text{ m s}^{-1}$ ) or using B-L, especially for BOMEX and RF01 (Table 1). The agreements of  $N_d$  with the LES results are best using the dynamics-PDF scheme, followed by the fixed  $\sigma_w$  ( $\sigma_w=0.7\text{ m s}^{-1}$ ) and B-L (Fig. 3 and Table 1). The best agreement using the dynamics-PDF scheme highlights the significance of the sub-grid variability of vertical velocity and the capability of the dynamics-PDF scheme to characterize it.

To illustrate the variability of vertical velocity, we show probability density function (PDF) of the vertical velocity ( $w$ ) over the last hour for BOMEX, RF01, and ATEX in Fig. 4. Three heights have been selected: cloud base where the droplet activation process occurs, the middle of the cloud layers, and cloud top. Note that the heights where the cloud layers are located vary among three cases. For the cumulus case of

BOMEX, the PDFs of  $w$  are positively skewed, with a tail extending towards positive larger values (Fig. 4a, b, and c). The positive skewness is realistic characteristic of cumulus clouds, updraft cores surrounded by a large area of weak downdrafts (LeMone, 1989; Moeng and Rotunno, 1990). The skewness is indicative of turbulent structure, but difficult to capture especially in large-scale models. The dynamics-PDF scheme is able to qualitatively characterize this positive skewness, although it is not quantitatively comparable with the COAMPS LES. The Gaussian distribution of the fixed  $\sigma_w$  ( $\sigma_w=0.7 \text{ m s}^{-1}$ ) approach has zero skewness and excessively large variance. The lack of positive skewness likely explains the underestimation of  $N_d$  (Fig. 3a and b).

In contrast to the cumulus case, the stratocumulus case of RF01 exhibits little skewness (Fig. 4d, e, and f). The PDFs of  $w$  tend to be symmetric around  $w=0 \text{ m s}^{-1}$ . The vertical velocity varies from  $-1.5 \text{ m s}^{-1}$  to  $1.5 \text{ m s}^{-1}$ , consistent with small vertical velocities observed in stratocumulus clouds (Stevens et al., 2005). The PDFs near cloud base are similar to those in the middle of cloud, but differ from those near cloud top. The variance of the fixed  $\sigma_w$  distribution is comparable to the LES in the lower and middle portion of the cloud layer, but too large near cloud top. In the intermediate case of ATEX, the PDFs of  $w$  are similar to those in BOMEX, except that  $w$  spans over a slightly wider range (Fig. 4g, h, and i).

To illustrate the impact of the sub-grid variability of the vertical velocity on aerosol activation, we show the probability density function (PDF) of the activated droplet number concentration ( $N_{\text{act}}$ ) near cloud bases over the last hour for BOMEX, RF01, and ATEX (Fig. 5). We present results with the sulfate aerosol concentrations  $m_a$  of  $1.0 \mu\text{g m}^{-3}$  and  $5.0 \mu\text{g m}^{-3}$ . For  $m_a=1.0 \mu\text{g m}^{-3}$ ,  $N_{\text{act}}$  spans a range from  $30 \text{ cm}^{-3}$  to  $100 \text{ cm}^{-3}$ , and peaks around  $60 \text{ cm}^{-3}$ . For  $m_a=5.0 \mu\text{g m}^{-3}$ ,  $N_{\text{act}}$  spans a wider range from  $60 \text{ cm}^{-3}$  to  $200 \text{ cm}^{-3}$ , and has multiple peaks. These peaks are partly due to discrete formulation of activation parameterization, (look-up tables are used to calculate  $N_{\text{act}}$ ), and partly due to the nonlinear dependence of aerosol activation on vertical velocity, aerosol concentrations, and others.

**Dynamics-PDF in  
GFDL SCM-CLUBB**

H. Guo et al.

Title Page

Abstract

Introduction

Conclusions

References

Tables

Figures

◀

▶

◀

▶

Back

Close

Full Screen / Esc

Printer-friendly Version

Interactive Discussion



Sub-grid variability of vertical velocity is significant, and varies for different cloud types and with height. The dynamics-PDF scheme is capable of qualitatively capturing the sub-grid variability of vertical velocity. Ignoring the sub-grid variability or simplifying it to be a constant produces less accurate estimates of droplet number concentration (Fig. 3).

In order to gain some insights of the aerosol effects on cloud optical properties, we conducted an offline calculation of cloud optical depth ( $\tau$ ) over the last hour for three cases. The cloud optical depths, for  $m_a=1.0 \mu\text{g m}^{-3}$  and  $5.0 \mu\text{g m}^{-3}$ , are 0.52 and 0.70 in BOMEX, 7.7 and 10.0 in RF01, and 6.4 and 8.2 in ATEX. Generally, the optical depth increases by  $\sim 30\%$  as  $m_a$  increases from  $1.0 \mu\text{g m}^{-3}$  to  $5.0 \mu\text{g m}^{-3}$ . Furthermore, the cloud albedo ( $\alpha_c$ ) for non-absorbing and homogeneous clouds can be approximated as a function of  $\tau$ ,  $\alpha_c = \frac{\tau}{\tau+7.7}$ , following Lacis and Hansen (1974). So a back-of-the-envelope estimate of  $\alpha_c$  of the stratocumulus cloud in RF01 would increase from 0.50 to 0.57 as  $m_a$  increases by a factor of 5.

#### 4 Concluding remarks and future work

The use of a multi-variate probability density function (dynamics-PDF) of moisture, temperature, and vertical velocity to parameterize cloud fraction, condensate, and droplet number is promising. The profiles for cloud properties in GFDL-CLUBB compare favorably with those from the COAMPS large eddy simulations (LES) as well as with available observations. The good agreement between the GFDL SCM-CLUBB simulations and the COAMPS LES has been achieved without any case-specific adjustments. This uniform treatment of the planetary boundary layer should benefit global simulations where a variety of regimes exist. The good agreement between the SCM-CLUBB simulations, LES, and observations for cloud fraction and cloud water is consistent with earlier results (Golaz et al., 2002b). Moreover, for the first time, the successful simulation of cloud droplet number concentration from the GFDL SCM-CLUBB has been achieved.

## Dynamics-PDF in GFDL SCM-CLUBB

H. Guo et al.

Title Page

Abstract

Introduction

Conclusions

References

Tables

Figures



Back

Close

Full Screen / Esc

Printer-friendly Version

Interactive Discussion



**Dynamics-PDF in  
GFDL SCM-CLUBB**

H. Guo et al.

[Title Page](#)[Abstract](#)[Introduction](#)[Conclusions](#)[References](#)[Tables](#)[Figures](#)[I◀](#)[▶I](#)[◀](#)[▶](#)[Back](#)[Close](#)[Full Screen / Esc](#)[Printer-friendly Version](#)[Interactive Discussion](#)

We have also conducted both low and high vertical resolution simulations. Our findings indicate that a hybrid configuration is feasible, where the dynamics-PDF scheme uses relatively high resolution while the SCM uses relatively low resolution, and they communicate through linear interpolation. This hybrid configuration can generally approximate well the results using high resolution in both the dynamics-PDF parameterization and the SCM. The cloud profiles in the low and high resolution simulations are qualitatively similar, and their magnitude differences generally remain within ~30%.

Ultimately, one motivation for developing this parameterization for cloud droplet number concentration is to assess how aerosols impact droplet number and the radiative, microphysical, and macrophysical properties of clouds, including their albedo, areas, and life times. These issues will be addressed more thoroughly in future research. Future research will

1. evaluate the dynamics-PDF parameterization for cases with mixed phase clouds, deep and shallow convection, and precipitation;
2. incorporate a two-moment microphysical package with the dynamics-PDF parameterization, and explore the aerosol-cloud interactions within a more realistic and self-consistent framework;
3. deploy the dynamics-PDF parameterization in a full GCM configuration, and evaluate its performance for simulating global climatology and cloud properties.

**Appendix A****High and Low Resolution SCM-CLUBB Simulations**

In the high vertical resolution SCM-CLUBB simulations (i.e., dynamics-PDF (high-res)), the vertical spacing is 40 m in the lowest 2 km and then stretched upwards for the host SCM. 101 vertical levels are used to represent a vertical domain from the surface to

40 km. The vertical levels for the dynamics-PDF scheme overlap those for the host SCM in the lowest 4 km (Fig. A1). The time step is 3 min for both the host SCM and the dynamics-PDF scheme. Such set-ups might be challenging with available computer power for current global climate simulations.

In the low vertical resolution SCM-CLUBB simulations (i.e., dynamics-PDF (low-res)), we coarsen the vertical spacing for the host SCM but remain relatively refined vertical spacing for the dynamics-PDF scheme. The vertical spacing is 150 m in the lowest 2 km and total 67 vertical levels are used for the host SCM; the vertical spacing for the dynamics-PDF scheme is  $\frac{1}{3}$  of that for the host SCM in the lowest 4 km, because each vertical layer in the host SCM is evenly divided into three sub-layers that are used for the dynamics-PDF scheme (Fig. A1). The communication between the host SCM and the dynamics-PDF scheme is realized via linear interpolation into sub-layers. The time steps are 30 min and 3 min for the host SCM and for the dynamics-PDF scheme, respectively. Hence, 10 substeps are used in the dynamics-PDF scheme in order to march forward one time step in the host SCM.

*Acknowledgements.* H. Guo is supported by the grant GC08-249, Climate Prediction Program for the Americas (CPPA), NOAA Climate Program Office. V. E. Larson, D. P. Schanen, and B. M. Griffin acknowledge support by grant ATM-0936186 from the National Science Foundation and by grant NA09OAR4310123 from NOAA.

## References

- Boucher, O. and Lohmann, U.: The sulfate-CCN-cloud albedo effect: A sensitivity study with two general circulation models, *Tellus B*, 47, 281–300, 1995.
- Donner, L. J., Seman, C. J., and Hemler, R. S.: Three-dimensional cloud-system modeling of GATE convection, *J. Atmos. Sci.*, 56, 1885–1912, 1999.
- Donner, L. J., Wyman, B. L., Hemler, R. S., et al.: The dynamical core, physical parameterizations, and basic simulation characteristics of the atmospheric component of the GFDL global coupled model CM3, *J. Climate*, to be submitted, 2010.

## Dynamics-PDF in GFDL SCM-CLUBB

H. Guo et al.

Title Page

Abstract

Introduction

Conclusions

References

Tables

Figures

◀

▶

◀

▶

Back

Close

Full Screen / Esc

Printer-friendly Version

Interactive Discussion



- Forster, P., Ramaswamy, V., Artaxo, P., et al.: Changes in Atmospheric Constituents and in Radiative Forcing. In: Climate Change 2007: The Physical Science Basis, in: Contribution of Working Group I to the Fourth Assessment Report of the Intergovernmental Panel on Climate Change, edited by: Solomon, S., Qin, D., Manning, M., Chen, Z., Marquis, M., Averyt, K. B., Tignor, M., and Miller, H. L., Cambridge University Press, Cambridge, United Kingdom and New York, NY, USA, 2007.
- Ghan, S. J., Leung, L. R., Easter, R. C., and Abdul-Razzak, H.: Prediction of cloud droplet number in a general circulation model, *J. Geophys. Res.*, 102, 21777–21794, 1997.
- Golaz, J.-C.: A PDF-based parameterization for boundary layer clouds, Ph.D. thesis, Colorado State University, Fort Collins, CO, 125 pp., 2001.
- Golaz, J.-C., Larson, V. E., and Cotton, W. R.: A PDF based model for boundary layer clouds. Part I: Method and model description, *J. Atmos. Sci.*, 59, 3540–3551, 2002a.
- Golaz, J.-C., Larson, V. E., and Cotton, W. R.: A PDF based model for boundary layer clouds. Part II: Model results, *J. Atmos. Sci.*, 59, 3552–3571, 2002b.
- Golaz, J.-C., Wang, S., Doyle, J. D., and Schmidt, J. M.: COAMPS<sup>®</sup>-LES: Model evaluation and analysis of second and third moment vertical velocity budgets, *Bound.-Lay. Meteorol.*, 116, 487–517, 2005.
- Golaz, J.-C., Larson, V. E., Hansen, J. A., Schanen, D. P., and Griffin, B. M.: Elucidating model inadequacies in a cloud parameterization by use of an ensemble-based calibration framework, *Mon. Weather Rev.*, 135, 4077–4096, 2007.
- Golaz, J.-C., Salzman, M., and Donner, L. J.: Sensitivity to upscaling assumptions of the sub-grid cloud drop activation in the GFDL AM3 GCM, in preparation, 2010.
- Heintzenberg, J. and Charlson, R. J.: Clouds in the perturbed climate system, MIT press, 2009.
- Lacis, A. A. and Hansen, J. E.: A parameterization for the absorption of solar radiation in the earth's atmosphere, *J. Atmos. Sci.*, 31, 118–133, 1974.
- Lappen, C.-L. and Randall, D. A.: Toward a unified parameterization of the boundary layer and moist convection. Part I: A new type of mass-flux model, *J. Atmos. Sci.*, 58, 2021–2036, 2001.
- Larson, V.-E., Golaz, J.-C., and Cotton, W. R.: Small-scale and mesoscale variability in cloudy boundary layers: Joint probability density function, *J. Atmos. Sci.*, 59, 3519–3539, 2002.
- Larson, V. E. and Golaz, J.-C.: Using probability density functions to derive consistent closure relationships among higher-order moments, *Mon. Weather Rev.*, 133, 1023–1042, 2005.

**Dynamics-PDF in  
GFDL SCM-CLUBB**

H. Guo et al.

[Title Page](#)[Abstract](#)[Introduction](#)[Conclusions](#)[References](#)[Tables](#)[Figures](#)[◀](#)[▶](#)[◀](#)[▶](#)[Back](#)[Close](#)[Full Screen / Esc](#)[Printer-friendly Version](#)[Interactive Discussion](#)

**Dynamics-PDF in  
GFDL SCM-CLUBB**

H. Guo et al.

[Title Page](#)[Abstract](#)[Introduction](#)[Conclusions](#)[References](#)[Tables](#)[Figures](#)[◀](#)[▶](#)[◀](#)[▶](#)[Back](#)[Close](#)[Full Screen / Esc](#)[Printer-friendly Version](#)[Interactive Discussion](#)

- Leary, C. A. and Houze Jr., R. A.: The contribution of mesoscale motions to the mass and heat fluxes of an intense tropical convective system, *J. Atmos. Sci.*, 37, 784–796, 1980.
- LeMone, M. A.: Some observations of vertical velocity skewness in the convective planetary boundary layer, *J. Atmos. Sci.*, 47, 1163–1169, 1989.
- 5 Lohmann, U., Feichter, J., Chuang, C. C., and Penner, J. E.: Prediction of the number of cloud droplets in the ECHAM GCM, *J. Geophys. Res.*, 104, 9169–9198, 1999.
- Mellor, G. L.: The Gaussian cloud model relations, *J. Atmos. Sci.*, 34, 356–358, 1977.
- Moeng, C.-H. and Rotunno, R.: Vertical-velocity skewness in the buoyancy-driven boundary layer, *J. Atmos. Sci.*, 47, 1149–1162, 1990.
- 10 Ming, Y., Ramaswamy, V., Donner, L. J., and Phillips, V. T. J.: A new parameterization of cloud droplet activation applicable to General Circulation Models, *J. Atmos. Sci.*, 63, 1348–1356, 2006.
- Ming, Y., Ramaswamy, V., Donner, L. J., Phillips, V. T. J., Klein, S. A., Ginoux, P. A., and Horowitz, L. W.: Modeling the interactions between aerosol and liquid water clouds with a self-consistent cloud scheme in a General Circulation Model, *J. Atmos. Sci.*, 64, 1189–1209, 2007.
- 15 Morrison, H. and Gettelman, A.: A new two-moment bulk stratiform cloud microphysics scheme in the Community Atmosphere Model, Version 3 (CAM3). Part I: Description and numerical tests, *J. Climate*, 21, 3642–3659, 2008.
- 20 Ovtchinnikov, M. and Ghan, S. J.: Parallel simulations of aerosol influence on clouds using cloud-resolving and single-column models, *J. Geophys. Res.*, 110, D15S10, doi:10.1029/2004JD005088, 2005.
- Ramanathan, V., Crutzen, P. J., Kiehl, J. T., and Rosenfeld, D.: Aerosols, climate, and the hydrological cycle, *Science*, 294, 2119–2124, 2001.
- 25 Randall, D. A.: Conditional instability of the first kind upside-down, *J. Atmos. Sci.*, 37, 125–130, 1980.
- Randall, D. A., Curry, J., Dwyer, P., Krueger, S., et al.: The second GEWEX Cloud Systems Study science and implementation plan, International GEWEX Project Office Series No. 34, 45 pp., International GEWEX Project Office, 1010 Wayne Ave., Suite 450, Silver Spring, MD 20910, 2000.
- 30 Siebesma, A. P., Bretherton, C. S., Brown, A., et al.: A large-eddy simulation intercomparison study of shallow cumulus convection, *J. Atmos. Sci.*, 60, 1201–1219, 2003.

**Dynamics-PDF in  
GFDL SCM-CLUBB**

H. Guo et al.

[Title Page](#)[Abstract](#)[Introduction](#)[Conclusions](#)[References](#)[Tables](#)[Figures](#)[I◀](#)[▶I](#)[◀](#)[▶](#)[Back](#)[Close](#)[Full Screen / Esc](#)[Printer-friendly Version](#)[Interactive Discussion](#)

Stevens, B., Feingold, G., Cotton, W. R., and Walko, R. L.: Elements of the microphysical structure of numerically simulated nonprecipitating stratocumulus, *J. Atmos. Sci.*, 53, 980–1006, 1996.

Stevens, B., Ackerman, A. S., Albrecht, B. A., et al.: Simulations of trade-wind cumuli under a strong inversion, *J. Atmos. Sci.*, 58, 1870–1891, 2001.

Stevens, B., Moeng, C.-H., Ackerman, A. S., et al.: Evaluation of large-eddy simulations via observations of nocturnal marine stratocumulus, *Mon. Weather Rev.*, 133, 1443–1462, 2005.

Stull, R. B.: An introduction to boundary layer meteorology, Kluwer Academic Publishers, 1988.

Webb, M. J., Senior, C. A., Sexton, D. M. H., et al.: On the contribution of local feedback mechanisms to the range of climate sensitivity in two GCM ensembles, *Clim. Dynam.*, 27, 17–38, 2006.

Zhu, P., Bretherton, C. S., Köhler, M., et al.: Intercomparison and interpretation of single column model simulations of a nocturnal stratocumulus topped marine boundary layer, *Mon. Weather Rev.*, 133, 2741–2758, 2005.

Dynamics-PDF in  
GFDL SCM-CLUBB

H. Guo et al.

**Table 1.** The time and space averaged in-cloud cloud droplet number concentrations ( $N_d$ ,  $\text{cm}^{-3}$ ) using dynamics-PDF scheme, fixed standard deviation of vertical velocity ( $\sigma_w$ ), B-L (Boucher and Lohmann, 1995) scheme in low resolution single column model simulations, and reference large eddy simulations (LES) with the sulfate mass concentrations ( $m_a$ ) of  $1.0 \mu\text{g m}^{-3}$  and  $5.0 \mu\text{g m}^{-3}$ .

		$N_d$ ( $\text{cm}^{-3}$ )		fixed $\sigma_w$		B-L
		LES	dynamics-PDF	$\sigma_w=0.7 \text{ m s}^{-1}$	$\sigma_w=2.0 \text{ m s}^{-1}$	
$m_a=1.0 \mu\text{g m}^{-3}$	BOMEX	78.4	72.7 (−7%) <sup>1</sup>	45.2 (−42%)	64.9 (−17%)	162 (+106%)
	RF01	72.6	70.4 (−3%)	48.4 (−33%)	69.5 (−4%)	162 (+123%)
	ATEX	71.4	91.1 (+28%)	51.4 (−28%)	73.8 (+3%)	162 (+127%)
$m_a=5.0 \mu\text{g m}^{-3}$	BOMEX	183.3	175.4 (−4%)	104.2 (−43%)	152.2 (−17%)	314 (+71%)
	RF01	173.9	153.9 (−11%)	111.6 (−36%)	163.0 (−6%)	314 (+81%)
	ATEX	159.3	207.9 (+31%)	118.4 (−26%)	173.0 (+9%)	314 (+97%)

<sup>1</sup> Values in parentheses are the relative differences with respect to the reference LES results.

Title Page

Abstract

Introduction

Conclusions

References

Tables

Figures

◀

▶

◀

▶

Back

Close

Full Screen / Esc

Printer-friendly Version

Interactive Discussion



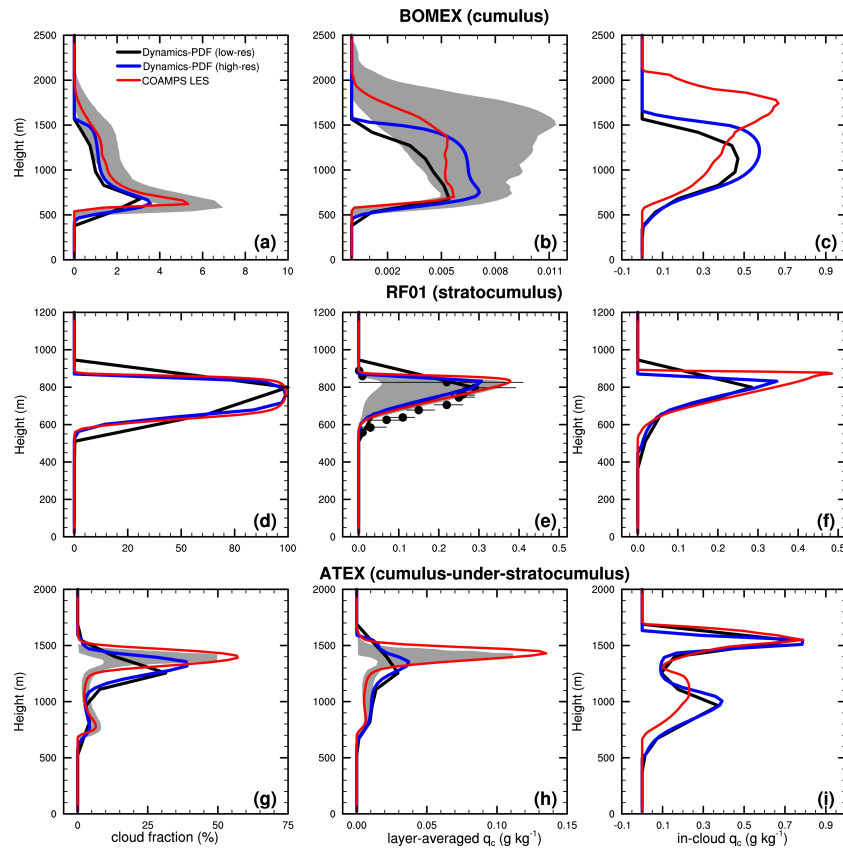


**Fig. 1.** Comparison of the cloud fraction, layer-averaged, and in-cloud cloud water content ( $q_c$ ) profiles from the GFDL SCM-CLUBB simulations with the dynamic multi-variate probability density function (dynamics-PDF) scheme using high (blue) and low (black) vertical resolutions (denoted as dynamics-PDF (high-res) and dynamics-PDF (low-res), respectively), and from the COAMPS LES (large eddy simulation) (red), for three cases of BOMEX in (a), (b), (c), RF01 in (d), (e), (f), and ATEX in (g), (h), (i). Shaded areas indicate the range (upper and lower bounds) of the LES ensemble from the LES comparison studies. Dots in (e) indicate averages of observed values, and horizontal bars in (e) indicate the first and third quartiles of the observed values (Zhu et al., 2005).

Title Page

Abstract

Introduction

Conclusions

References

Tables

Figures

◀

▶

◀

▶

Back

Close

Full Screen / Esc

Printer-friendly Version

Interactive Discussion



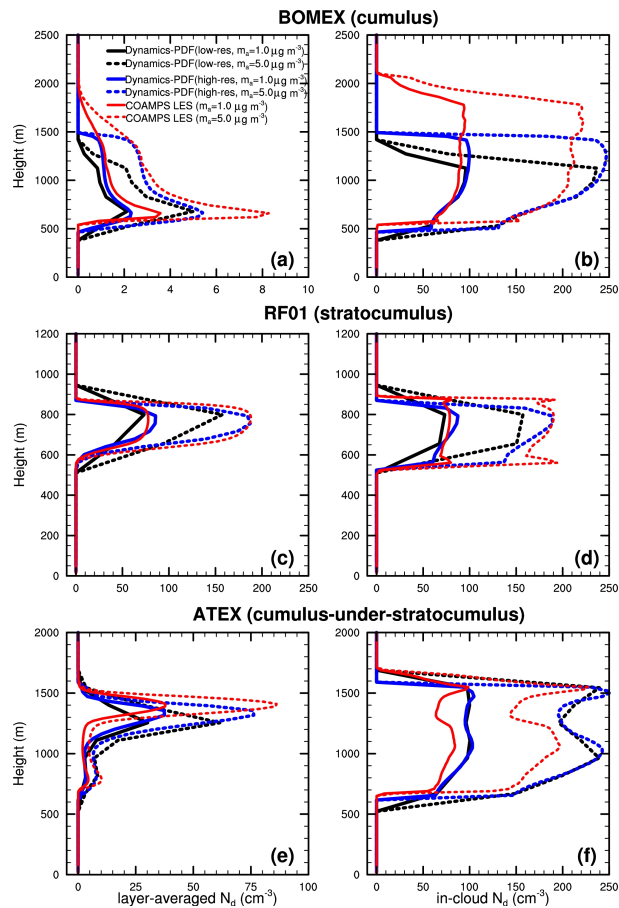


**Fig. 2.** Similar to Fig. 1, but for the layer-averaged cloud droplet number concentration ( $N_d$ ) and the in-cloud  $N_d$  with sulfate aerosol mass concentrations ( $m_a$ ) of  $1.0 \mu\text{g m}^{-3}$  (solid) and of  $5.0 \mu\text{g m}^{-3}$  (dotted), respectively.

Title Page

Abstract

Introduction

Conclusions

References

Tables

Figures

◀

▶

◀

▶

Back

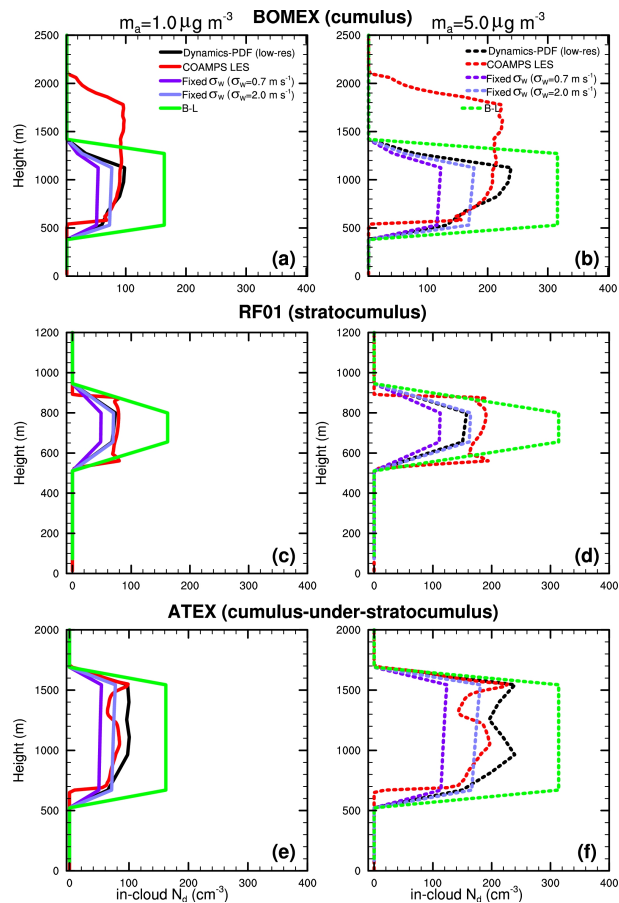
Close

Full Screen / Esc

Printer-friendly Version

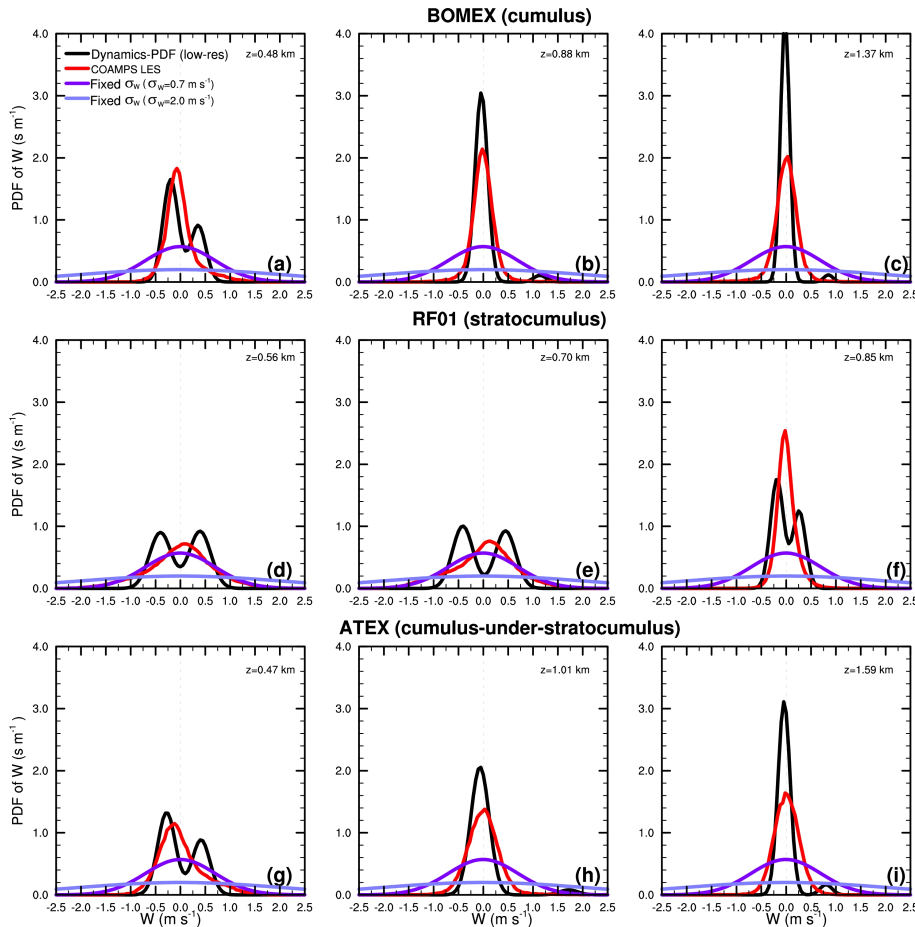
Interactive Discussion





**Fig. 3.** Profiles of in-cloud droplet number concentrations ( $N_d$ ) with sulfate aerosol mass concentrations ( $m_a$ ) of  $1.0 \mu\text{g m}^{-3}$  in (a), (c), and (e), and of  $5.0 \mu\text{g m}^{-3}$  in (b), (d), and (f), for three cases of BOMEX, RF01, and ATEX.

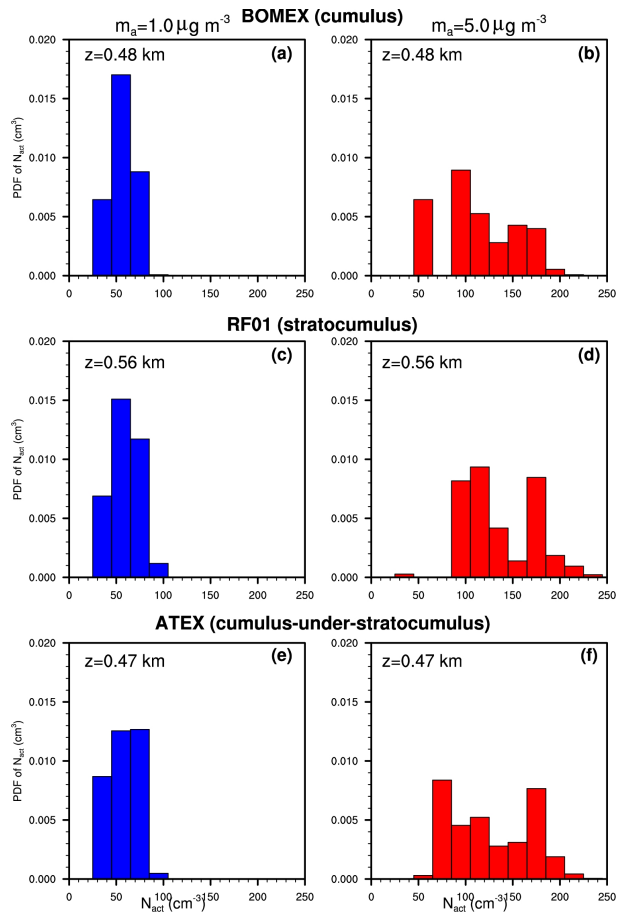
[Title Page](#)
[Abstract](#)
[Introduction](#)
[Conclusions](#)
[References](#)
[Tables](#)
[Figures](#)
[⏪](#)
[⏩](#)
[◀](#)
[▶](#)
[Back](#)
[Close](#)
[Full Screen / Esc](#)
[Printer-friendly Version](#)
[Interactive Discussion](#)

**Fig. 4.** Probability density function (PDF) of vertical velocity ( $w$ ) over the last hour near cloud bases in **(a)**, **(d)**, and **(g)**, in the middle of cloud layers in **(b)**, **(e)**, and **(h)**, and near cloud tops in **(c)**, **(f)**, and **(i)**, for three cases of BOMEX, RF01, and ATEX.

[Title Page](#)  
[Abstract](#)   [Introduction](#)  
[Conclusions](#)   [References](#)  
[Tables](#)   [Figures](#)  
[◀](#)   [▶](#)  
[◀](#)   [▶](#)  
[Back](#)   [Close](#)  
[Full Screen / Esc](#)  
[Printer-friendly Version](#)  
[Interactive Discussion](#)





**Fig. 5.** Probability density function (PDF) of the activated droplet number concentration ( $N_{\text{act}}$ ) over the last hour near cloud bases with sulfate aerosol mass concentrations ( $m_a$ ) of  $1.0 \mu\text{g m}^{-3}$  (blue) and of  $5.0 \mu\text{g m}^{-3}$  (red) for BOMEX in (a) and (b), RF01 in (c) and (d), and ATEX in (e) and (f).

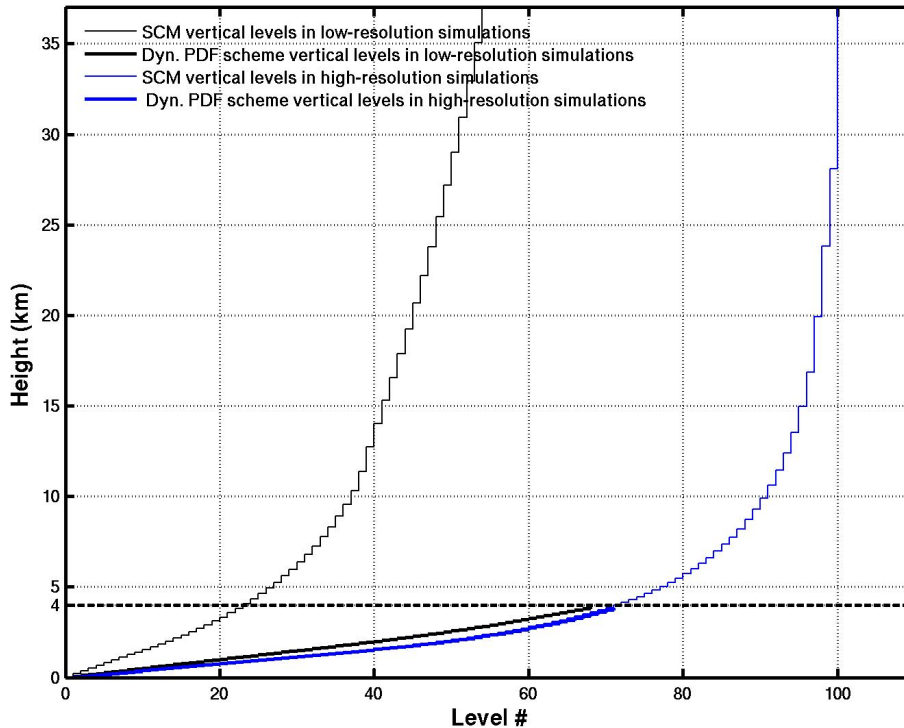


**Fig. A1.** Vertical distribution of grid levels for the single column model (SCM) and for the dynamic multi-variate probability density function (dynamics-PDF) scheme in the low- and high-resolution simulations. The dynamics-PDF scheme is applied in the lowest 4 km of the atmosphere (below the black dashed line). In the low resolution simulations, the vertical spacing for the dynamics-PDF scheme is  $\frac{1}{3}$  of that for the SCM (black solid curves). In the high resolution simulations, the vertical spacing for the dynamics-PDF scheme is the same as that for the SCM, and so the vertical levels overlap below 4 km (blue solid curves).

Title Page

Abstract

Introduction

Conclusions

References

Tables

Figures

◀

▶

◀

▶

Back

Close

Full Screen / Esc

Printer-friendly Version

Interactive Discussion

